DOE/NV/11718--367

Atmospheric correction algorithm for hyperspectral imagery

Lee C. Sanders,[a] Rolando V. Raqueño,[a] and John R. Schott[a]

[a]Rochester Institute of Technology, Rochester, New York, USA
in collaboration with the
Department of Energy, Remote Sensing Laboratory, Las Vegas, Nevada, USA

ABSTRACT

In December 1997, the U.S. Department of Energy (DOE) established a Center of Excellence (Hyperspectral-Multispectral Algorithm Research Center, HyMARC) for promoting the research and development of algorithms to exploit spectral imagery. This center is located at the DOE Remote Sensing Laboratory in Las Vegas, Nevada, and is operated for the DOE by Bechtel Nevada. This paper presents the results to date of a research project begun at the center during 1998 to investigate the correction of hyperspectral data for atmospheric aerosols.

Results of a project conducted by the Rochester Institute of Technology to define, implement, and test procedures for absolute calibration and correction of hyperspectral data to absolute units of high spectral resolution imagery will be presented. Hybrid techniques for atmospheric correction using image or spectral scene data coupled through radiative propagation models will be specifically addressed. Results of this effort to analyze HYDICE sensor data will be included. Preliminary results based on studying the performance of standard routines, such as Atmospheric Pre-corrected Differential Absorption and Nonlinear Least Squares Spectral Fit, in retrieving reflectance spectra show overall reflectance retrieval errors of approximately one to two reflectance units in the 0.4- to 2.5-micron-wavelength region (outside of the absorption features). These results are based on HYDICE sensor data collected from the Southern Great Plains Atmospheric Radiation Measurement site during overflights conducted in July of 1997. Results of an upgrade made in the model-based atmospheric correction techniques, which take advantage of updates made to the moderate resolution atmospheric transmittance model (MODTRAN 4.0) software, will also be presented. Data will be shown to demonstrate how the reflectance retrievals in the shorter wavelengths of the blue–green region will be improved because of enhanced modeling of multiple scattering effects.

1. INTRODUCTION

Radiometrically calibrated hyperspectral imagery contains information relating to the material properties of a surface target and the atmospheric layers between the surface target and the sensor. All atmospheric layers contain molecular gases, aerosol particles, and water vapor, and information about these constituents may be extracted from hyperspectral imagery by using specially designed algorithms. It then follows that these algorithms can be used to characterize the atmosphere in a reliable, radiative transfer program to estimate the spectral ground reflectance to aid in ground-cover classification. A modular approach that incorporates some of the existing algorithms for atmospheric characterization and includes some new techniques would be a welcome tool for recovering ground reflectance from hyperspectral sensor radiance values.

2. BACKGROUND

The radiative transfer terms for the total inversion algorithm are derived by MODTRAN 4.0[1] and calculated for a user-defined range of surface elevations (pressure-depth), aerosol loadings (visibility), and columnar water-vapor amounts (cwv). The radiometric parameters are stored in a 3-D Look-Up Table (LUT) for use in the atmospheric correction process as well as in the different fitting routines discussed below. For the different inclusive techniques, the following radiative equations, using the conventions described by Schott in a 1997 publication,[2] can be selected:

$$L_{sensor} = \frac{\left(E_s \tau_1 \tau_2 \cos(\sigma)\pi^{-1} + L_{downwelled}\,\tau_2\right)\rho}{(1.0 - \rho_{avg} S)} + L_{upwelled} + \rho_{avg} L_{env} \tau_2 \qquad (1)$$

or

$$L_{sensor} = \frac{\left(E_s \tau_1 \tau_2 \cos(\sigma)\pi^{-1} + L_{downwelled}\,\tau_2\right)\rho}{(1.0 - \rho S)} + L_{upwelled} \qquad (2)$$

where L_{sensor} is the total radiance measured at the sensor by a detector element, $E_s t_1 t_2 cos(s) p^{-1}$ is the direct solar radiance including transmissive effects of the atmosphere, $L_{downwelled}\tau_{22}$ is the scattered atmospheric radiance onto the target including transmissive effects of the atmosphere, r is the surface reflectance of the target, r_{avg} is the average reflectance of the target surround, S is the spherical albedo of the atmosphere, L_u is the atmospheric upwelled radiance which has no target or surround interaction, $L_{env} t_2$ is the direct and scattered solar radiance that interacts with the surround (r_{avg}) and is scattered into the target-sensor path, τ_1 and τ_2 are respectively the sun target and target sensor transmissions, and σ is the solar declination angle (Figure 1). Equation 2 is included for the cases where the surround effect is assumed to be negligible, or the user has a LUT with only single-scattered radiometric terms. In order to invert Equation 1 or 2 to spectral reflectance, the variables (pressure-depth, visibility, and cwv) must be estimated for input in the radiative transfer process and then the radiative transfer terms (for Equation 1 or 2) can be extracted from the LUT previously described.

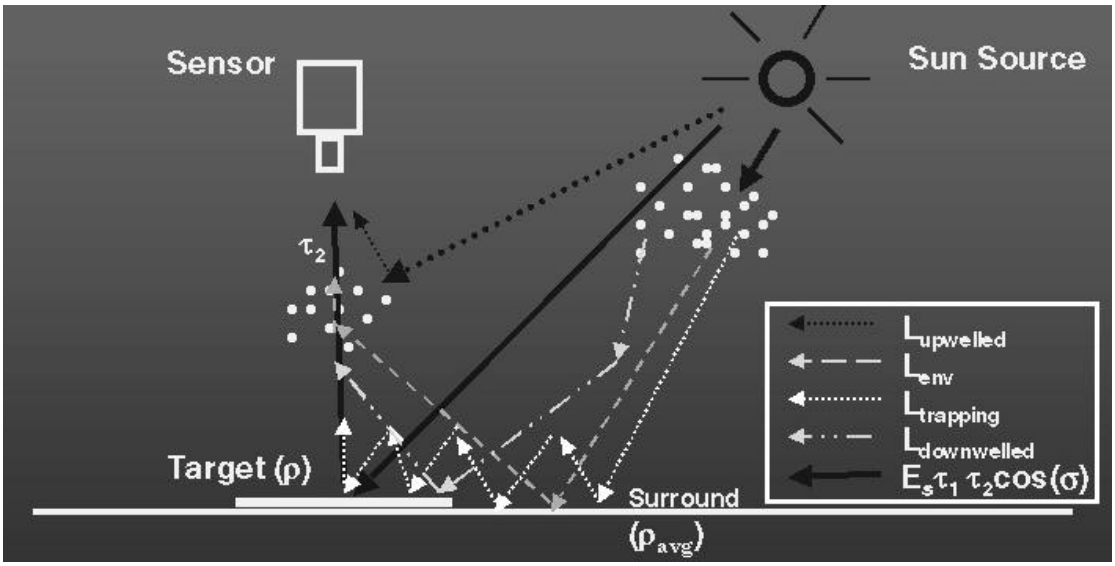

Figure 1. Scene model depicting the different radiative transfer paths

3. APPROACH

The following algorithms were used to characterize the atmospheric input variables as part of this total radiance-to-reflectance inversion program.

The Non-Linear Least Squared Spectral Fit (NLLSSF) technique was developed as a curve-fitting routine for atmospheric spectral features.[3] The assumption is that the reflectance is a linear function of wavelength with the exception of a non-linear scaling term to account for liquid water or chlorophyll. This technique fits the absorption feature for oxygen at 760 nm to estimate the surface-pressure depth profile of the scene. Once this parameter is fixed, the sensor radiance from 400 to 700 nm is fit to the radiative transfer model to derive the visibility or aerosol loading. The next step is to fit the 940 nm water vapor feature to extract the atmospheric cwv amount. Once all these parameters are fixed, the radiative transfer equation can be populated and then inverted to yield ground reflectance.

The Atmospheric Pre-Corrected Differential Absorption (APDA) technique was developed by Schläpfer, *et al.*,[4] to extract the atmospheric cwv using a simple band ratio method much like the continuum interpolated band ratio CIBR method[5,6] but with the added improvement of subtracting the estimated atmospheric upwelled radiance.

A new approach referred to as Regression Intersection Method for Aerosol Correction (RIMAC) was developed that uses the upwelled radiance values from the Regression Intersection Method[7,8] to estimate the visibility parameter for a selected aerosol type. This technique assumes that the majority of the upwelled radiance is a function of aerosol scattering properties in the 550- to 700-nm range. The advantage in using RIMAC is that it uses only in-scene data to derive the atmospheric visibility parameter. The overall relationships and flow of these various techniques is summarized in the diagram depicted in Figure 2.

A new numerical approximation technique was developed to calculate the effect of the target surround (L_{env}) on the sensor-received radiance (Figure 3). Once the aerosol loading and type are fixed, the corresponding phase function from the radiative transfer model can be used to estimate the contribution of each target surround pixel (Figure 4) to the observed radiance. Once the average reflectance (ρ_{avg}) of the surround is calculated, its contribution to the pixel of interest can be calculated and removed. This involves a simple, two-pass solution. In the first pass, the mean spectral reflectances are approximated with the assumption that the average reflectance (ρ_{avg}) equals the target reflectance (ρ). The second pass then utilizes Equation 1, as stated, to invert to reflectance.

To implement the total radiance-to-reflectance inversion algorithm, the user selects the options to be used for the atmospheric characterization (options include default values), provides the directory paths to the LUT and image(s), and chooses the radiative transfer equation (Equation 1 or 2). The output of the program is a reflectance cube of the same dimensions as the input image and an image information cube that holds all of the atmospheric characterization values. It should be noted that most of the solution(s) from the atmospheric characterization routines can be generated on a per pixel basis or over some averaging window (for noise reduction).

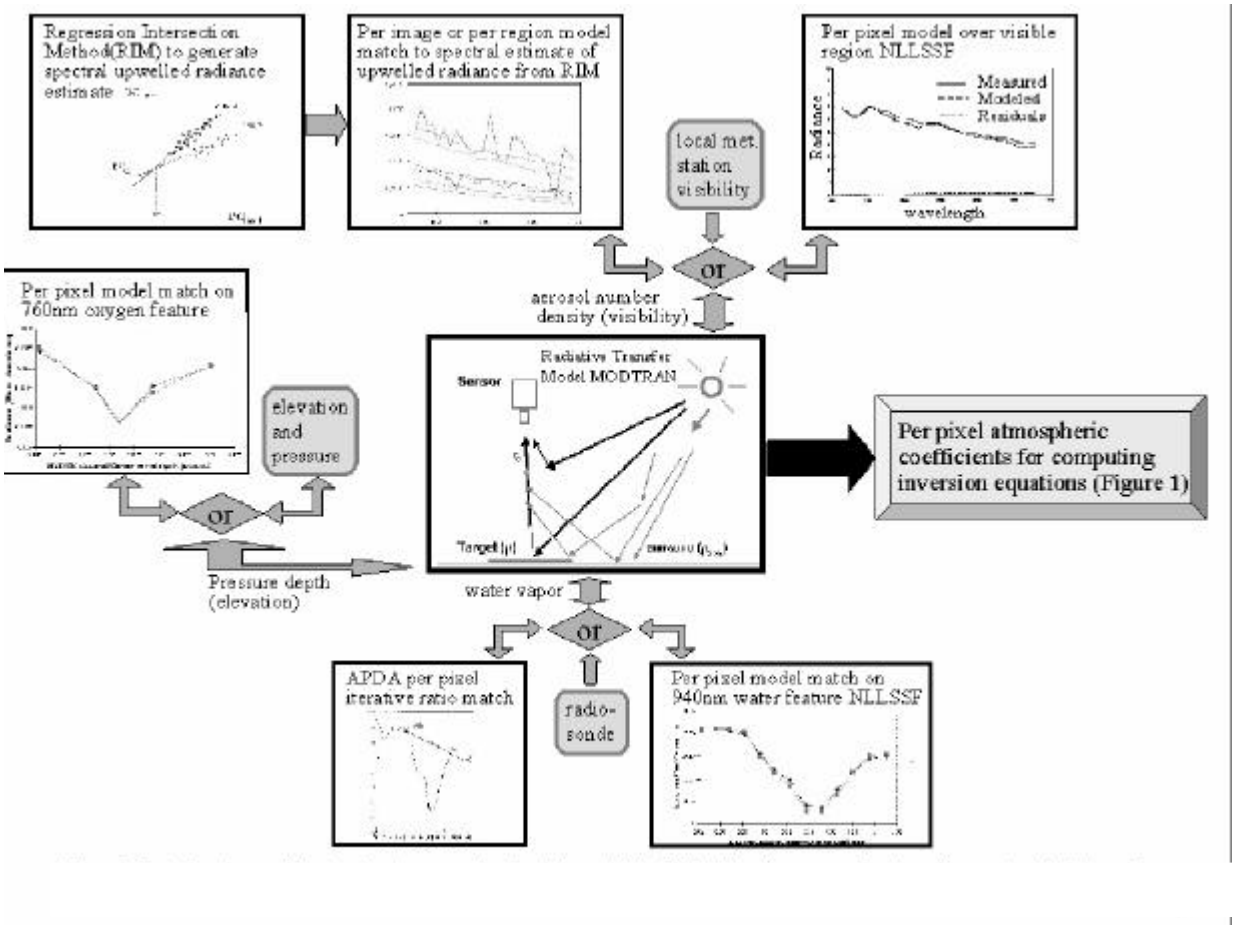

Figure 2. Atmospheric compensation algorithms available at RIT and how they are combined to perform atmospheric inversion.

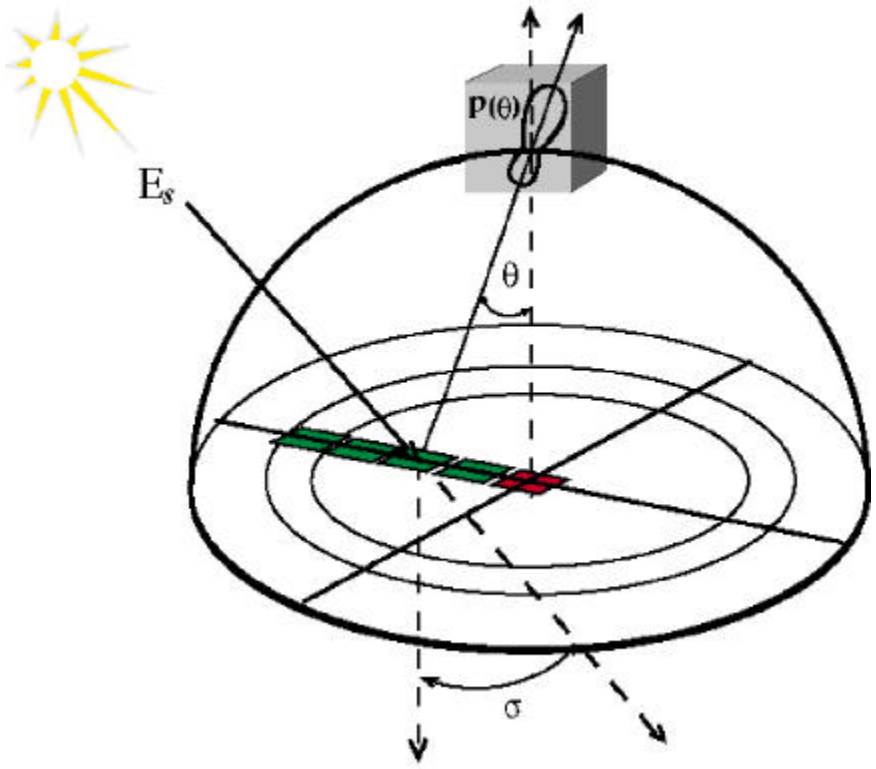

Figure 3. The contribution of surround-to-sensor scattering for a single atmospheric layer where p(λ, θ, i) is the scattering-phase function for the i^{th} atmospheric layer

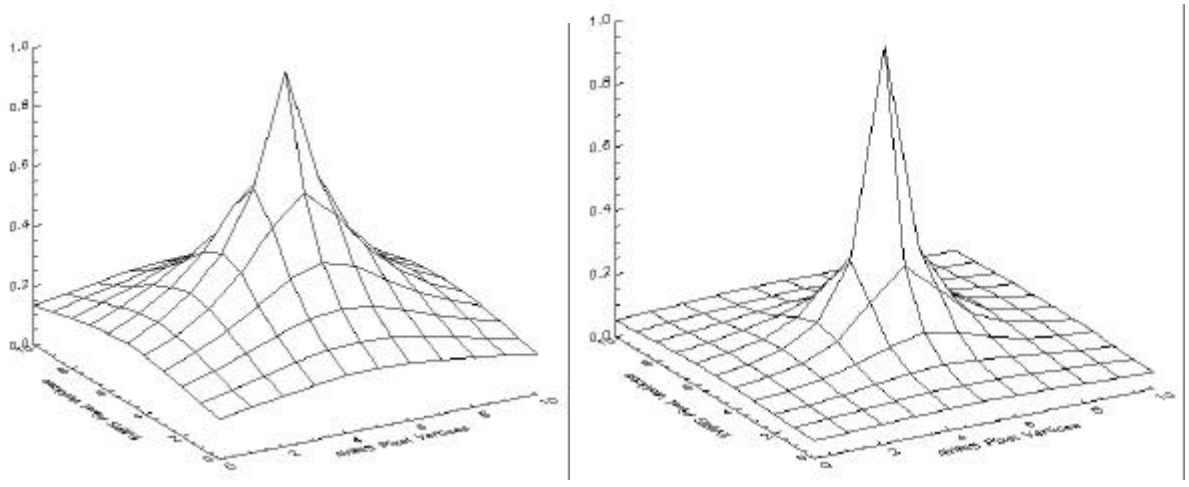

Figure 4. The relative contribution of surround radiance for the vertices of a ground-projected 11 x 11 AVIRIS grid in the 0.411-µm band (left) and the 1.748-µm band (right). The center vertex is the center of the target pixel

4. RESULTS

These atmospheric characterization and reflectance inversion tools were applied to a HYDICE data collection over the Department of Energy's Atmospheric Radiation Measurement Program (ARM) site. For this collection, several well-characterized reflective panels were deployed for ground truth as shown in Figure 5. These panels had nominal reflectance values of 2, 4, 8, 16, 32, and 64 percent. For evaluation purposes, the difference in reflectance in each band was computed for each panel. Figure 6 shows a plot of the nominal 32 percent reflector and the two-pass inverted reflectance for the same 32 percent reflectance target using the NLLSSF to recover cwv and pressure-depth and RIMAC to recover visibility. Also shown in this plot is the root mean square difference in reflectance in each band for the 2, 4, 8, 16, 32, and 64 percent panels using the single-pass and two-pass algorithms. Note that the water absorption bands have been zeroed out for clarity. The data showed a very good general pattern of agreement that deteriorates some toward the blue region and is quite poor long of 2.0 μm.

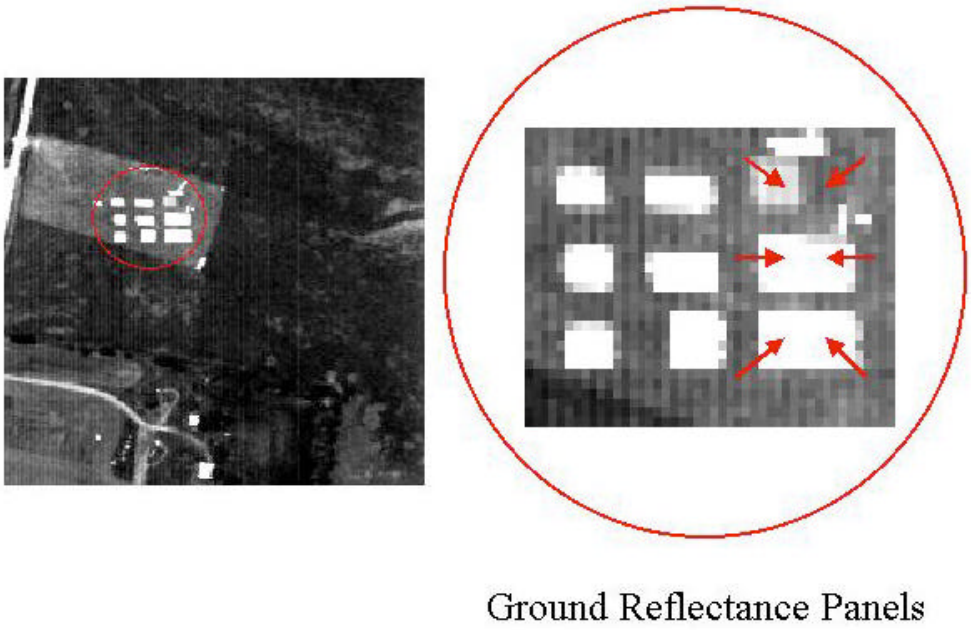

Figure 5. A HYDICE image of the ARMS site reflectance panels

The poor performance long of 2.0 μm may be due to instrument calibration errors in this region. Errors have been reported here, and a new calibration (which was used here) was generated by the HYDICE program. However, some concerns persist about the calibration in this region. We would not expect this type of anomaly due to errors in atmospheric parameters. The errors at the blue end of the spectrum were largely due to errors in the aerosol term. Figure 7 and Figure 8 shows the retrieved reflectance error for the various ground reflectance panels utilizing the first- and second-pass atmospheric correction processes, respectively. Note how the second-pass algorithm, which accounts for aerosol scattering from the surround, dramatically improved the errors in this region, though some error persisted. The fine spectral shape to the error is, we believe, largely due to differences between the instrument spectral calibration and the MODTRAN spectral radiometry models. With a more robust data set, we would expect these fine errors to show a consistent pattern that could be removed with a constant spectral correction term. This approach has proven effective with the AVIRIS instrument as reported by Green.[3]

When comparing different atmospheric correction approaches, two trends show up with the small data set studied here as shown in Figure 9. The different atmospheric characterization approaches all perform reasonably well and generate comparable errors. The default approach is simply the image-wide use of meteorological data as input to MODTRAN. This is a very best case scenario for this approach because the terrain and atmosphere were flat and very stable, and we had all the ARM site data to characterize the MODTRAN inputs. As a result, this should be treated as a very best case. The NLLSSF used Green's approach[3] as implemented at the Rochester Institute of Technology (RIT) for all MODTRAN inputs. The Def_RIMAC_NL used the local elevation to define pressure-depth, RIMAC to define visibility, and NLLSSF to define cwv.

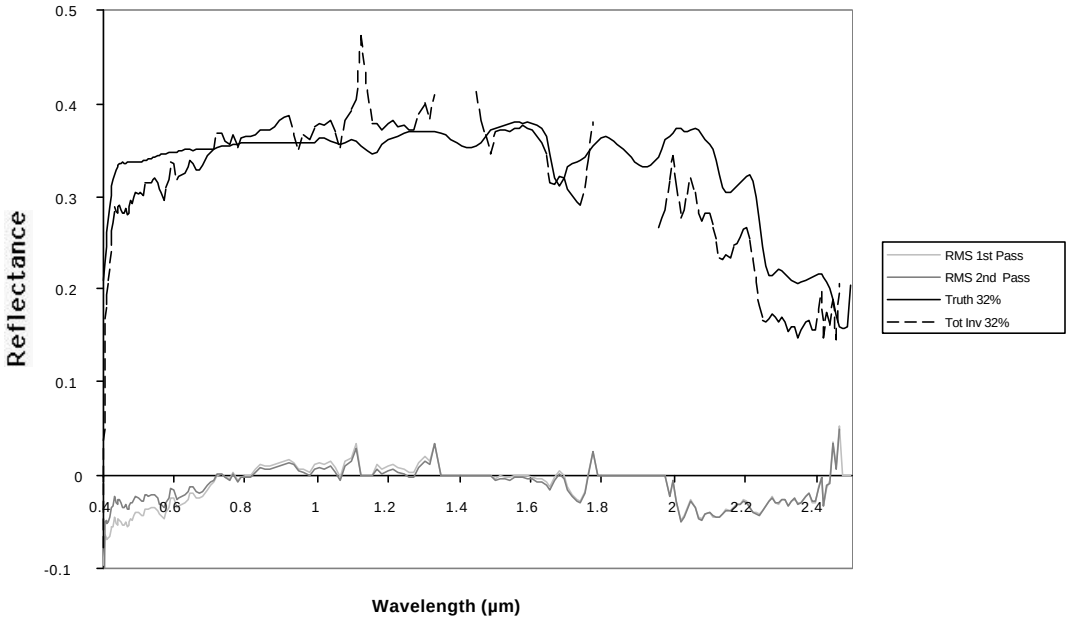

Figure 6. Comparison of inverted reflectance values and truth. The spectral reflectance of the nominal 32 percent reflector is shown as an example. The reflectance error plots are the average spectral RMS values of the difference between inverted and true reflectance for the 2, 4, 8, 16, 32, and 64 percent panels.

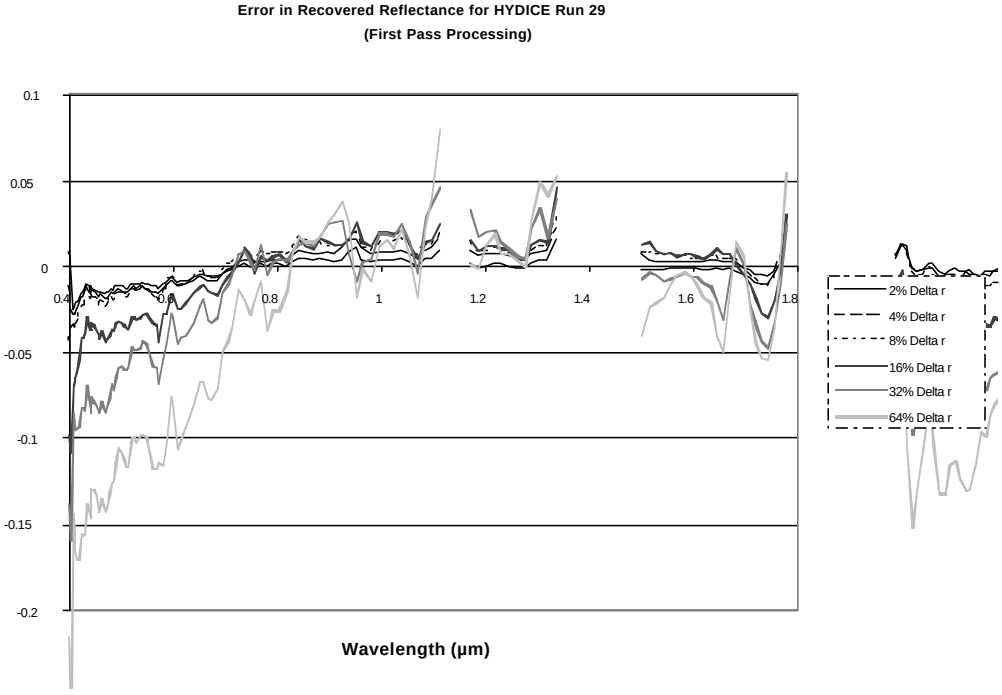

Figure 7. VIS/NIR spectrum error in recovered reflectance for ground target panels applying a first-pass atmospheric correction process (Def_RIMAC_NL)

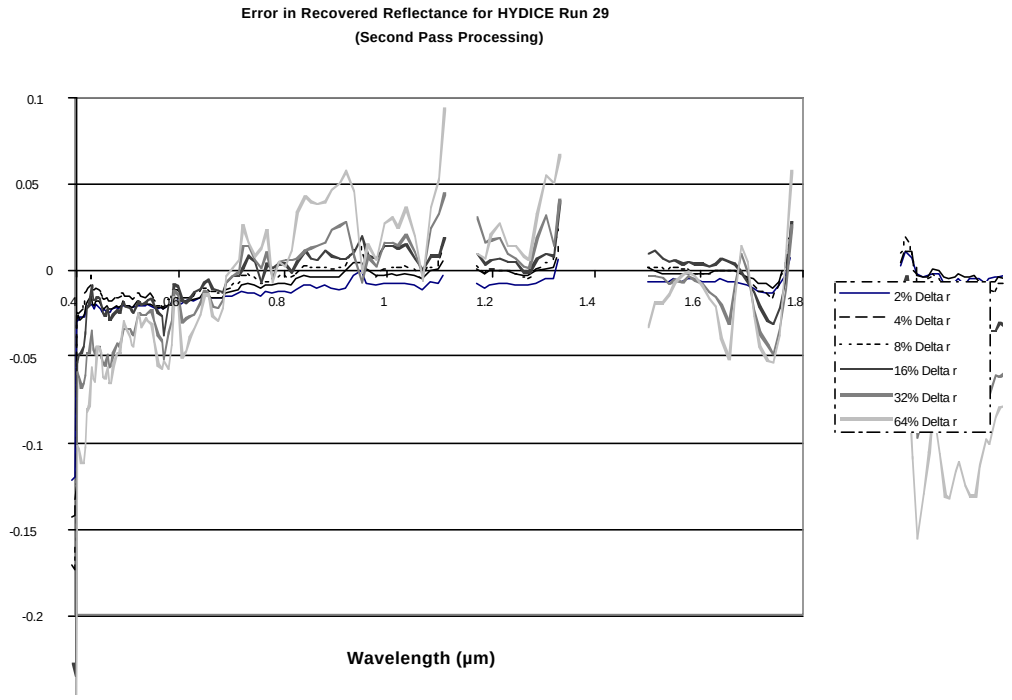

Figure 8. VIS/NIR spectrum error in recovered reflectance for ground target panels applying a second-pass atmospheric correction process (Def_RIMAC_NL)

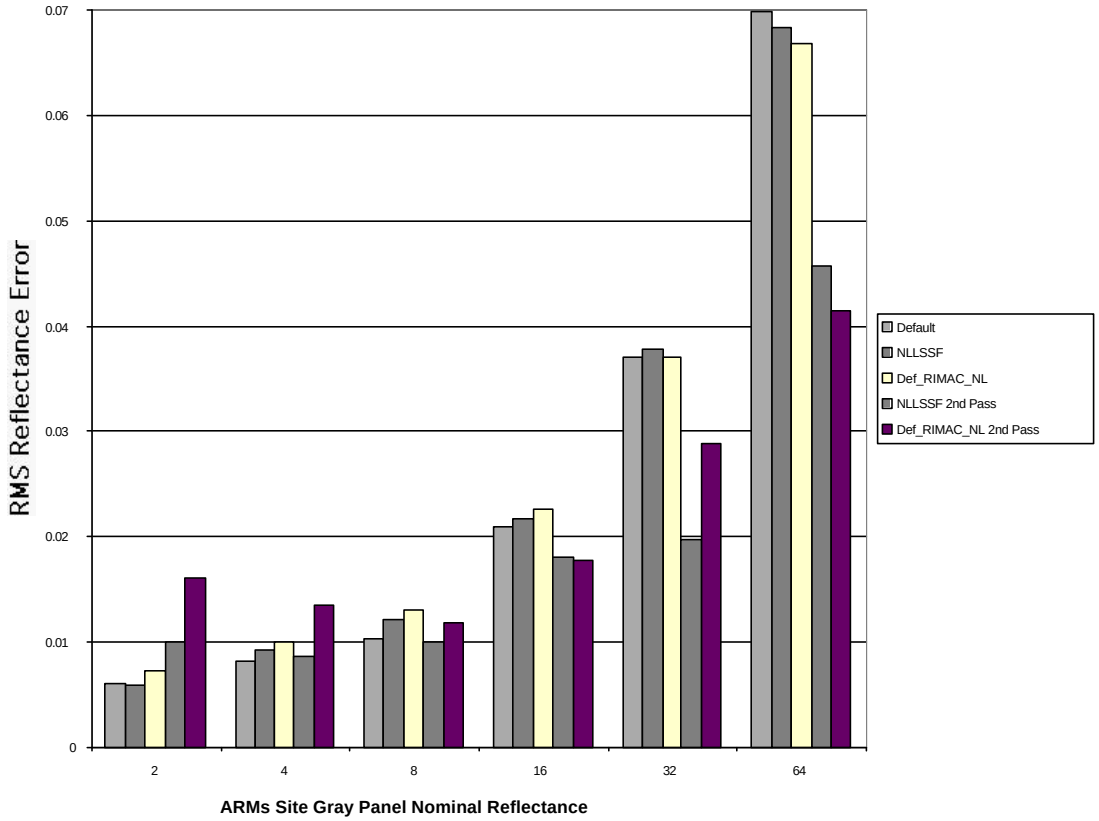

Figure 9. VIS/NIR spectrum RMS error in recovered reflectance for different atmospheric correction options

All of these estimation techniques can be used with essentially no interactive user input except a general estimate of the aerosol type. The most significant difference in the results from the initial comparison was a significant reduction in the errors when using the second-pass approach. This is most significant, as one would expect, for shorter wavelengths as shown in Figure 6 and Figure 8 and small higher contrast targets as shown for the brightest targets in Figure 9. The data set tested to date has not included a significant range of atmospheric or elevation conditioning to allow us to more robustly compare the model-matching techniques, all of which allow considerable promise. However, preliminary results have indicated that this approach is lending itself to compensating for cloud effects in the imagery. Initial results show promise in correcting for the additional scattered downwelled radiance from clouds and corresponding reduction in scattered downwelled sky radiance using model-matching algorithms.

5. ACKNOWLEDGEMENTS

This work was supported by the U.S. Department of Energy, Nevada Operations Office, under contract No. DE-AC08-96NV11718. By acceptance of this article, No. DOE/NV/11718--367, the publisher and/or recipient acknowledge the right of the U.S. government to retain a nonexclusive, royalty-free license in and to any copyright covering the article.

6. REFERENCES

1. A. Berk, L. S. Bernstein, and D. C. Robertson, "MODTRAN: a moderate resolution model for LOWTRAN 7," GL-TR-89-0122, Spectral Sciences, Burlington, MA, 1989.
2. J. R. Schott, *Remote Sensing: The Image Chain Approach*, Oxford University Press, 1997.
3. R. O. Green, D. A. Roberts, J. E. Conel, "Characterization and compensation of the atmosphere for the inversion of AVIRIS calibrated radiance to apparent surface reflectance," Preliminary AVIRIS Workshop.z **1**, Jet Propulsion Laboratory, 1996.
4. D. Schläpfer, C. Borel, J Keller, and K. Itten, "Atmospheric pre-corrected differential absorption technique to retrieve columnar water vapor," *Summaries of the Sixth Annual JPL Airborne Earth Science Workshop*. **1**, March 4, 1996.
5. R. O. Green, V. Carrére, and J. E. Conel, "Measurement of atmospheric water vapor using the airborne visible/infrared imaging spectrometer," *American Society of Photogrammetry and Remote Sensing*. Workshop Image Processing, Sparkes, Nevada, 1989.
6. C. J. Bruegge, J. E. Conel, J. S. Margolis, R. O. Green, G. Toon, V. Carrere, R. G. Holm, and G. Hoover, "In-situ atmospheric water-vapor retrieval in support of AVIRIS validation," *Imaging Spectroscopy of the Terrestrial Environment, SPIE Vol. 1298*. pp. 150-163, 1990.
7. R. E. Crippen, "The regression intersection method of adjusting image data for band ratioing," *International Journal of Remote Sensing*. **8**, No. 2, pp. 137-155, 1986.
8. L. R. Gaddis, L. A. Soderblom, H. H. Kieffer, K. J. Becker, J. Torson, and K. Mullins, "Decomposition of AVIRIS spectra: extraction of surface-reflectance, atmospheric, and instrumental components," *IEEE Transactions on Geoscience and Remote Sensing*. **34**, No. 1, pp. 163-177, 1996.

DISTRIBUTION

DOE Public Reading Facility	(1)
OSTI	(2)
TIRC	(1)